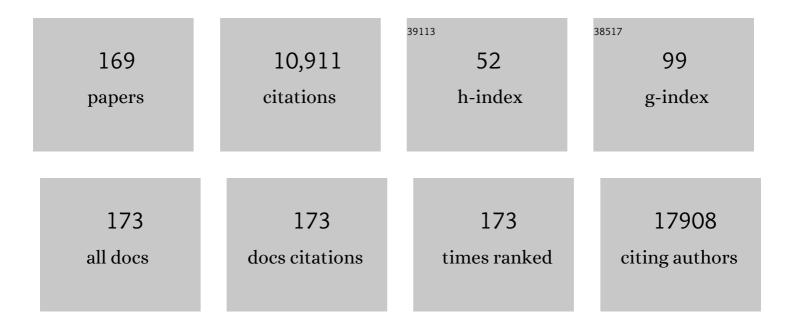
List of Publications by Year in descending order

Source: https://exaly.com/author-pdf/7896314/publications.pdf Version: 2024-02-01



WELNIEN SU

#	Article	IF	CITATIONS
1	Highly Reversible Zn Metal Anode Stabilized by Dense and Anionâ€Derived Passivation Layer Obtained from Concentrated Hybrid Aqueous Electrolyte. Advanced Functional Materials, 2022, 32, 2103959.	7.8	48
2	Surface-engineered N-doped carbon nanotubes with B-doped graphene quantum dots: Strategies to develop highly-efficient noble metal-free electrocatalyst for online-monitoring dissolved oxygen biosensor. Carbon, 2022, 186, 406-415.	5.4	36
3	Chemical stability of sulfide solid-state electrolytes: stability toward humid air and compatibility with solvents and binders. Energy and Environmental Science, 2022, 15, 991-1033.	15.6	100
4	Highly Active Oxygen Coordinated Configuration of Fe Singleâ€Atom Catalyst toward Electrochemical Reduction of CO <sub>2</sub> into Multi arbon Products. Advanced Functional Materials, 2022, 32, .	7.8	37
5	Synthesis of one-dimensional vanadium-doped CoS/Co9S8 heterojunctions as bifunctional electrocatalysts for zinc-air battery. Materials Today Energy, 2022, 25, 100968.	2.5	8
6	Heterostructured composite of NiFe-LDH nanosheets with Ti4O7 for oxygen evolution reaction. Materials Today Chemistry, 2022, 24, 100824.	1.7	10
7	Lithium nitrate as a surplus lithium source for anode-free cell with Ni-rich (NMC811) cathode. Journal of Power Sources, 2022, 532, 231303.	4.0	15
8	Resolving anodic and cathodic interface-incompatibility in solid-state lithium metal battery via interface infiltration of designed liquid electrolytes. Journal of Power Sources, 2022, 535, 231425.	4.0	9
9	Strategies towards High Performance Lithiumâ€Sulfur Batteries. Batteries and Supercaps, 2022, 5, .	2.4	30
10	Lithium Oxalate as a Lifespan Extender for Anode-Free Lithium Metal Batteries. ACS Applied Materials & Interfaces, 2022, 14, 26724-26732.	4.0	21
11	Evolution of Interfacial Phenomena Induced by Electrolyte Formulation and Hot Cycling of Anode-Free Li-Metal Batteries. ACS Applied Energy Materials, 2022, 5, 7770-7783.	2.5	8
12	Fibrous organosulfur cathode materials with high bonded sulfur for high-performance lithium-sulfur batteries. Journal of Power Sources, 2022, 541, 231693.	4.0	22
13	Engineering self-supported ruthenium-titanium alloy oxide on 3D web-like titania as iodide oxidation reaction electrocatalyst to boost hydrogen production. Applied Catalysis B: Environmental, 2022, 316, 121608.	10.8	16
14	Dilute dual-salt electrolyte for successful passivation of in-situ deposited Li anode and permit effective cycling of high voltage anode free batteries. Journal of Power Sources, 2022, 542, 231752.	4.0	3
15	Decoupling Interfacial Reactions at Anode and Cathode by Combining Online Electrochemical Mass Spectroscopy with Anodeâ€Free Liâ€Metal Battery. Advanced Functional Materials, 2021, 31, 2006951.	7.8	27
16	Highly-lithiophilic Ag@PDA-GO film to Suppress Dendrite Formation on Cu Substrate in Anode-free Lithium Metal Batteries. Energy Storage Materials, 2021, 35, 334-344.	9.5	91
17	Enhancing the electrochemical performance of a flexible solid-state supercapacitor using a gel polymer electrolyte. Materials Today Communications, 2021, 26, 102102.	0.9	15
18	New Insights into the N–S Bond Formation of a Sulfurized-Polyacrylonitrile Cathode Material for Lithium–Sulfur Batteries. ACS Applied Materials & Interfaces, 2021, 13, 14230-14238.	4.0	33

#	Article	IF	CITATIONS
19	Decoupling the origins of irreversible coulombic efficiency in anode-free lithium metal batteries. Nature Communications, 2021, 12, 1452.	5.8	111
20	Origin of shuttle-free sulfurized polyacrylonitrile in lithium-sulfur batteries. Journal of Power Sources, 2021, 492, 229508.	4.0	33
21	Effects of a Thermally Electrochemically Activated β-PVDF Fiber on Suppression of Li Dendrite Growth for Anode-Free Batteries. ACS Applied Energy Materials, 2021, 4, 3240-3248.	2.5	16
22	Bridging role of ethyl methyl carbonate in fluorinated electrolyte on ionic transport and phase stability for lithium-ion batteries. Journal of Power Sources, 2021, 494, 229760.	4.0	20
23	Synergistic Hybrid Support Comprising TiO <sub>2</sub> –Carbon and Ordered PdNi Alloy for Direct Hydrogen Peroxide Synthesis. ACS Catalysis, 2021, 11, 8407-8416.	5.5	22
24	lodide Oxidation Reaction Catalyzed by Ruthenium–Tin Surface Alloy Oxide for Efficient Production of Hydrogen and Iodine Simultaneously. ACS Sustainable Chemistry and Engineering, 2021, 9, 8803-8812.	3.2	14
25	Mitigating dendrite formation and electrolyte decomposition via functional double layers coating on copper current collector in anode-free lithium metal battery. Journal of the Taiwan Institute of Chemical Engineers, 2021, 128, 87-97.	2.7	15
26	Investigation into the development of lithium-ion battery electrolytes and related knowledge transfer using research paper-based social network analysis. Journal of Energy Storage, 2021, 41, 102890.	3.9	5
27	Guiding lithium-ion flux to avoid cell's short circuit and extend cycle life for an anode-free lithium metal battery. Journal of Power Sources, 2021, 506, 230204.	4.0	27
28	Tuning Dynamically Formed Active Phases and Catalytic Mechanisms of <i>In Situ</i> Electrochemically Activated Layered Double Hydroxide for Oxygen Evolution Reaction. ACS Nano, 2021, 15, 14996-15006.	7.3	56
29	Flexible hydrophobic filter paper-based SERS substrate using silver nanocubes for sensitive and rapid detection of adenine. Microchemical Journal, 2021, 168, 106349.	2.3	28
30	Plasmonic paper substrates for point-of-need applications: Recent developments and fabrication methods. Sensors and Actuators B: Chemical, 2021, 345, 130401.	4.0	16
31	Structural evolution and Au nanoparticles enhanced photocatalytic activity of sea-urchin-like TiO2 microspheres: An X-ray absorption spectroscopy study. Applied Surface Science, 2021, 562, 150127.	3.1	8
32	Exploring the performance of carbonate and ether-based electrolytes for anode-free lithium metal batteries operating under various conditions. Journal of Power Sources, 2021, 512, 230388.	4.0	6
33	Synergetic effect of water-in-bisalt electrolyte and hydrogen-bond rich additive improving the performance of aqueous batteries. Journal of Power Sources, 2021, 511, 230413.	4.0	19
34	Dual CuCl doped argyrodite superconductor to boost the interfacial compatibility and air stability for all solid-state lithium metal batteries. Nano Energy, 2021, 90, 106542.	8.2	53
35	Review of recent offshore wind power strategy in Taiwan: Onshore wind power comparison. Energy Strategy Reviews, 2021, 38, 100747.	3.3	13
36	A Powerful Protocol Based on Anode-Free Cells Combined with Various Analytical Techniques. Accounts of Chemical Research, 2021, 54, 4474-4485.	7.6	17

#	Article	IF	CITATIONS
37	Dielectric nanosheet modified plasmonic-paper as highly sensitive and stable SERS substrate and its application for pesticides detection. Spectrochimica Acta - Part A: Molecular and Biomolecular Spectroscopy, 2020, 225, 117484.	2.0	30
38	Binder-free ultra-thin graphene oxide as an artificial solid electrolyte interphase for anode-free rechargeable lithium metal batteries. Journal of Power Sources, 2020, 450, 227589.	4.0	93
39	Engineering heterometallic bonding in bimetallic electrocatalysts: towards optimized hydrogen oxidation and evolution reactions. Catalysis Science and Technology, 2020, 10, 893-903.	2.1	15
40	Mechanistic understanding of the Sulfurized-Poly(acrylonitrile) cathode for lithium-sulfur batteries. Energy Storage Materials, 2020, 26, 483-493.	9.5	99
41	Electrocatalytic reduction of carbon dioxide on gold–copper bimetallic nanoparticles: Effects of surface composition on selectivity. Electrochimica Acta, 2020, 356, 136756.	2.6	24
42	Multifunctional Properties of Al <sub>2</sub> O <sub>3</sub> /Polyacrylonitrile Composite Coating on Cu to Suppress Dendritic Growth in Anode-Free Li-Metal Battery. ACS Applied Energy Materials, 2020, 3, 7666-7679.	2.5	41
43	Ag nanocubes decorated 1T-MoS2 nanosheets SERS substrate for reliable and ultrasensitive detection of pesticides. Applied Materials Today, 2020, 21, 100871.	2.3	29
44	Ultrathin Li <sub>6.75</sub> La <sub>3</sub> Zr <sub>1.75</sub> Ta <sub>0.25</sub> O <sub>12</sub> -Based Composite Solid Electrolytes Laminated on Anode and Cathode Surfaces for Anode-free Lithium Metal Batteries. ACS Applied Energy Materials, 2020, 3, 11713-11723.	2.5	35
45	Resolving the Phase Instability of a Fluorinated Ether, Carbonate-Based Electrolyte for the Safe Operation of an Anode-Free Lithium Metal Battery. ACS Applied Energy Materials, 2020, 3, 10722-10733.	2.5	26
46	A new high-Li <sup>+</sup> -conductivity Mg-doped Li <sub>1.5</sub> Al <sub>0.5</sub> Ge <sub>1.5</sub> (PO <sub>4</sub> ) <sub>3</sub> solid electrolyte with enhanced electrochemical performance for solid-state lithium metal batteries. Journal of Materials Chemistry A, 2020, 8, 26055-26065.	5.2	25
47	Al–Sc dual-doped LiGe <sub>2</sub> (PO <sub>4</sub> ) <sub>3</sub> – a NASICON-type solid electrolyte with improved ionic conductivity. Journal of Materials Chemistry A, 2020, 8, 11302-11313.	5.2	36
48	Dual-Doped Cubic Garnet Solid Electrolytes with Superior Air Stability. ACS Applied Materials & Interfaces, 2020, 12, 25709-25717.	4.0	55
49	Reliable and sensitive detection of pancreatic cancer marker by gold nanoflower-based SERS mapping immunoassay. Microchemical Journal, 2020, 158, 105099.	2.3	24
50	Morphology engineering of cobalt embedded in nitrogen doped porous carbon as bifunctional oxygen electrocatalyst for Zn-air battery. Materials Today Energy, 2020, 17, 100455.	2.5	12
51	Scalable Synthesis of Micron Size Crystals of CH 3 NH 3 PbI 3 at Room Temperature in Acetonitrile via Rapid Reactive Crystallization. ChemistrySelect, 2020, 5, 3266-3271.	0.7	1
52	Electrochemical transformation reaction of Cu–MnO in aqueous rechargeable zinc-ion batteries for high performance and long cycle life. Journal of Materials Chemistry A, 2020, 8, 17595-17607.	5.2	93
53	Garnet–PVDF composite film modified lithium manganese oxide cathode and sulfurized carbon anode from polyacrylonitrile for lithium-ion batteries. Journal of Materials Chemistry A, 2020, 8, 14043-14053.	5.2	12
54	Search for the Developing Trends by Patent Analysis: A Case Study of Lithium-Ion Battery Electrolytes. Applied Sciences (Switzerland), 2020, 10, 952.	1.3	11

#	Article	IF	CITATIONS
55	Roles of film-forming additives in diluted and concentrated electrolytes for lithium metal batteries: A density functional theory-based approach. Electrochemistry Communications, 2020, 113, 106685.	2.3	10
56	Hierarchical 3D Architectured Ag Nanowires Shelled with NiMn-Layered Double Hydroxide as an Efficient Bifunctional Oxygen Electrocatalyst. ACS Nano, 2020, 14, 1770-1782.	7.3	145
57	Effect of diethyl carbonate solvent with fluorinated solvents as electrolyte system for anode free battery. Journal of Power Sources, 2020, 461, 228102.	4.0	26
58	Developing high-voltage carbonate-ether mixed electrolyte via anode-free cell configuration. Journal of Power Sources, 2020, 461, 228053.	4.0	37
59	High-Rate and Long-Cycle Stability with a Dendrite-Free Zinc Anode in an Aqueous Zn-Ion Battery Using Concentrated Electrolytes. ACS Applied Energy Materials, 2020, 3, 4499-4508.	2.5	95
60	Effects of Concentrated Salt and Resting Protocol on Solid Electrolyte Interface Formation for Improved Cycle Stability of Anode-Free Lithium Metal Batteries. ACS Applied Materials & Interfaces, 2019, 11, 31962-31971.	4.0	58
61	Effect of bifunctional additive potassium nitrate on performance of anode free lithium metal battery in carbonate electrolyte. Journal of Power Sources, 2019, 437, 226912.	4.0	86
62	A review of transition metalâ€based bifunctional oxygen electrocatalysts. Journal of the Chinese Chemical Society, 2019, 66, 829-865.	0.8	82
63	Nucleation and Growth Mechanism of Lithium Metal Electroplating. Journal of the American Chemical Society, 2019, 141, 18612-18623.	6.6	144
64	Li7La2.75Ca0.25Zr1.75Nb0.25O12@LiClO4 composite film derived solid electrolyte interphase for anode-free lithium metal battery. Electrochimica Acta, 2019, 325, 134825.	2.6	54
65	Investigation of Sodium Plating and Stripping on a Bare Current Collector with Different Electrolytes and Cycling Protocols. ACS Applied Materials & Interfaces, 2019, 11, 39746-39756.	4.0	21
66	A new class of lithium-ion battery using sulfurized carbon anode from polyacrylonitrile and lithium manganese oxide cathode. Journal of Power Sources, 2019, 434, 126641.	4.0	13
67	Immobilized Single Molecular Molybdenum Disulfide on Carbonized Polyacrylonitrile for Hydrogen Evolution Reaction. ACS Nano, 2019, 13, 6720-6729.	7.3	40
68	Dual electrolyte additives of potassium hexafluorophosphate and tris (trimethylsilyl) phosphite for anode-free lithium metal batteries. Electrochimica Acta, 2019, 316, 52-59.	2.6	70
69	Concentrated Dual-Salt Electrolyte to Stabilize Li Metal and Increase Cycle Life of Anode Free Li-Metal Batteries. Journal of the Electrochemical Society, 2019, 166, A1501-A1509.	1.3	104
70	Synergetic electrocatalytic activities towards hydrogen peroxide: Understanding the ordered structure of PdNi bimetallic nanocatalysts. Electrochemistry Communications, 2019, 101, 93-98.	2.3	12
71	A wireless and redox mediator-free Z-scheme twin reactor for the separate evolution of hydrogen and oxygen. Materials Today Energy, 2019, 12, 208-214.	2.5	6
72	Locally Concentrated LiPF <sub>6</sub> in a Carbonate-Based Electrolyte with Fluoroethylene Carbonate as a Diluent for Anode-Free Lithium Metal Batteries. ACS Applied Materials & Interfaces, 2019, 11, 9955-9963.	4.0	141

#	Article	IF	CITATIONS
73	Improved bi-functional ORR and OER catalytic activity of reduced graphene oxide supported ZnCo2O4 microsphere. International Journal of Hydrogen Energy, 2019, 44, 1565-1578.	3.8	83
74	Sulfurizedâ^'poly(acrylonitrile) wrapped carbon sulfur composite cathode material for high performance rechargeable lithium sulfur batteries. Journal of Power Sources, 2019, 412, 670-676.	4.0	38
75	Site Activity and Population Engineering of NiRu-Layered Double Hydroxide Nanosheets Decorated with Silver Nanoparticles for Oxygen Evolution and Reduction Reactions. ACS Catalysis, 2019, 9, 117-129.	5.5	103
76	Selective and Low Overpotential Electrochemical CO2 Reduction to Formate on CuS Decorated CuO Heterostructure. Catalysis Letters, 2019, 149, 860-869.	1.4	36
77	Multilayer-graphene-stabilized lithium deposition for anode-Free lithium-metal batteries. Nanoscale, 2019, 11, 2710-2720.	2.8	118
78	Conversion of Carbon Dioxide into Valuable Chemicals through Electrochemical Reduction Using Transition Metal Electrocatalysts. ECS Meeting Abstracts, 2019, , .	0.0	0
79	New 2.1 V Lithium- Ion Battery with Sulfurized Polyacrylonitrile (SPAN) Anode and LiMn2O4 Cathode. ECS Meeting Abstracts, 2019, , .	0.0	0
80	Synergistic Effect of Cycling Strategies and Electrolyte for Effective Plating/Stripping of Anode Free Li Metal Batteries ECS Meeting Abstracts, 2019, , .	0.0	0
81	The Combined Effect of Cycling Strategy and Potential Electrolyte in Fast Charging/Discharging of Li-Metal Based Batteries. ECS Meeting Abstracts, 2019, , .	0.0	0
82	Sulfurized-Poly(acrylonitrile) Coated C/S Composite Cathode Materials for Rechargeable Lithium-Sulfur Batteries. ECS Meeting Abstracts, 2019, , .	0.0	0
83	Universal Mechanism and Rate Equation for Hydrogen Oxidation Reaction. ECS Meeting Abstracts, 2019, , .	0.0	0
84	Fibrous Organosulfur Compounds As Cathode Materials for High-Performance Lithium-Sulfur Batteries. ECS Meeting Abstracts, 2019, , .	0.0	0
85	Transition-Metal-Doped TiO2 Decorated Nife Layered Double Hydroxide Catalyst in Alkaline Oxygen Evolution Reaction. ECS Meeting Abstracts, 2019, , .	0.0	0
86	Robust and conductive MagnéliÂPhase Ti4O7 decorated on 3D-nanoflower NiRu-LDH as high-performance oxygen reduction electrocatalyst. Nano Energy, 2018, 47, 309-315.	8.2	59
87	Polyethylene oxide film coating enhances lithium cycling efficiency of an anode-free lithium-metal battery. Nanoscale, 2018, 10, 6125-6138.	2.8	215
88	<i>In situ</i> analytical techniques for battery interface analysis. Chemical Society Reviews, 2018, 47, 736-851.	18.7	355
89	Nanostructured nickel ferrite embedded in reduced graphene oxide for electrocatalytic hydrogen evolution reaction. Materials Today Energy, 2018, 8, 118-124.	2.5	47
90	In Situ Confined Synthesis of Ti <sub>4</sub> O <sub>7</sub> Supported Platinum Electrocatalysts with Enhanced Activity and Stability for the Oxygen Reduction Reaction. ChemCatChem, 2018, 10, 1155-1165.	1.8	20

#	Article	IF	CITATIONS
91	Descriptor study by density functional theory analysis for the direct synthesis of hydrogen peroxide using palladium–gold and palladium–mercury alloy catalysts. Molecular Systems Design and Engineering, 2018, 3, 896-907.	1.7	8
92	Synergy between Ceria Oxygen Vacancies and Cu Nanoparticles Facilitates the Catalytic Conversion of CO <sub>2</sub> to CO under Mild Conditions. ACS Catalysis, 2018, 8, 12056-12066.	5.5	137
93	Copper and Copperâ€Based Bimetallic Catalysts for Carbon Dioxide Electroreduction. Advanced Materials Interfaces, 2018, 5, 1800919.	1.9	72
94	Visible-Light-Mediated Electrocatalytic Activity in Reduced Graphene Oxide-Supported Bismuth Ferrite. ACS Omega, 2018, 3, 5946-5957.	1.6	74
95	3D-functionalized shell isolated Ag nanocubes on a miniaturized flexible platform for sensitive and selective SERS detection of small molecules. Microchemical Journal, 2018, 142, 305-312.	2.3	18
96	Designed Synergetic Effect of Electrolyte Additives to Improve Interfacial Chemistry of MCMB Electrode in Propylene Carbonate-Based Electrolyte for Enhanced Low and Room Temperature Performance. ACS Applied Materials & Interfaces, 2018, 10, 25252-25262.	4.0	31
97	Improvement of Cycling Performance of Na <sub>2/3</sub> Co <sub>2/3</sub> Mn <sub>1/3</sub> O <sub>2</sub> Cathode by PEDOT/PSS Surface Coating for Na Ion Batteries. Indonesian Journal of Chemistry, 2018, 18, 127.	0.3	1
98	Highly sensitive and stable Ag@SiO2 nanocubes for label-free SERS-photoluminescence detection of biomolecules. Spectrochimica Acta - Part A: Molecular and Biomolecular Spectroscopy, 2017, 175, 239-245.	2.0	27
99	A Plasmonic Coupling Substrate Based on Sandwich Structure of Ultrathin Silicaâ€Coated Silver Nanocubes and Flowerâ€Like Aluminaâ€Coated Etched Aluminum for Sensitive Detection of Biomarkers in Urine. Advanced Healthcare Materials, 2017, 6, 1601290.	3.9	11
100	Tuning/exploiting Strong Metal-Support Interaction (SMSI) in Heterogeneous Catalysis. Journal of the Taiwan Institute of Chemical Engineers, 2017, 74, 154-186.	2.7	238
101	Controllable embedding of sulfur in high surface area nitrogen doped three dimensional reduced graphene oxide by solution drop impregnation method for high performance lithium-sulfur batteries. Journal of Power Sources, 2017, 353, 298-311.	4.0	71
102	Revealing the mitigation of intrinsic structure transformation and oxygen evolution in a layered Li1.2Ni0.2Mn0.6O2 cathode using restricted charging protocols. Journal of Power Sources, 2017, 359, 539-548.	4.0	38
103	Visualization of Lithium Plating and Stripping via <i>in Operando</i> Transmission X-ray Microscopy. Journal of Physical Chemistry C, 2017, 121, 7761-7766.	1.5	123
104	Capacity retention of lithium sulfur batteries enhanced with nano-sized TiO <sub>2</sub> -embedded polyethylene oxide. Journal of Materials Chemistry A, 2017, 5, 6708-6715.	5.2	66
105	Tuning metal support interactions enhances the activity and durability of TiO2-supported Pt nanocatalysts. Electrochimica Acta, 2017, 224, 452-459.	2.6	101
106	Improved Interfacial Properties of MCMB Electrode by 1-(Trimethylsilyl)imidazole as New Electrolyte Additive To Suppress LiPF <sub>6</sub> Decomposition. ACS Applied Materials & Interfaces, 2017, 9, 2410-2420.	4.0	72
107	Dual onfined Sulfur in Hybrid Nanostructured Materials for Enhancement of Lithiumâ€&ulfur Battery Cathode Capacity Retention. ChemElectroChem, 2017, 4, 636-647.	1.7	31
108	DFT study reveals geometric and electronic synergisms of palladium-mercury alloy catalyst used for hydrogen peroxide formation. Applied Catalysis A: General, 2017, 547, 69-74.	2.2	16

#	Article	IF	CITATIONS
109	Identification of the physical origin behind disorder, heterogeneity, and reconstruction and their correlation with the photoluminescence lifetime in hybrid perovskite thin films. Journal of Materials Chemistry A, 2017, 5, 21002-21015.	5.2	10
110	Sequentially surface modified hematite enables lower applied bias photoelectrochemical water splitting. Physical Chemistry Chemical Physics, 2017, 19, 20881-20890.	1.3	34
111	Design of transition-metal-doped TiO <sub>2</sub> as a multipurpose support for fuel cell applications: using a computational high-throughput material screening approach. Molecular Systems Design and Engineering, 2017, 2, 449-456.	1.7	10
112	Ag@SiO <sub>2</sub> nanocube loaded miniaturized filter paper as a hybrid flexible plasmonic SERS substrate for trace melamine detection. Analytical Methods, 2017, 9, 6823-6829.	1.3	22
113	Platinum loaded on dual-doped TiO2 as an active and durable oxygen reduction reaction catalyst. NPG Asia Materials, 2017, 9, e403-e403.	3.8	43
114	Unravelling Surface Composition of Bimetallic Nanoparticles. ChemNanoMat, 2016, 2, 117-124.	1.5	6
115	Visible light responsive noble metal-free nanocomposite of V-doped TiO2 nanorod with highly reduced graphene oxide forÂenhanced solar H2 production. International Journal of Hydrogen Energy, 2016, 41, 6752-6762.	3.8	30
116	Hybrid nanostructured microporous carbon-mesoporous carbon doped titanium dioxide/sulfur composite positive electrode materials for rechargeable lithium-sulfur batteries. Journal of Power Sources, 2016, 324, 239-252.	4.0	57
117	Interplay between Molybdenum Dopant and Oxygen Vacancies in a TiO <sub>2</sub> Support Enhances the Oxygen Reduction Reaction. ACS Catalysis, 2016, 6, 6551-6559.	5.5	103
118	Resilient Yolk–Shell Silicon–Reduced Graphene Oxide/Amorphous Carbon Anode Material from a Synergistic Dual oating Process for Lithiumâ€ion Batteries. ChemElectroChem, 2016, 3, 1446-1454.	1.7	25
119	Facile Synthesis of [101]-Oriented Rutile TiO <sub>2</sub> Nanorod Array on FTO Substrate with a Tunable Anatase–Rutile Heterojunction for Efficient Solar Water Splitting. ACS Sustainable Chemistry and Engineering, 2016, 4, 5963-5971.	3.2	53
120	A highly stable CuS and CuS–Pt modified Cu <sub>2</sub> O/CuO heterostructure as an efficient photocathode for the hydrogen evolution reaction. Journal of Materials Chemistry A, 2016, 4, 2205-2216.	5.2	199
121	Using hematite for photoelectrochemical water splitting: a review of current progress and challenges. Nanoscale Horizons, 2016, 1, 243-267.	4.1	612
122	Rational design of ethanol steam reforming catalyst based on analysis of Ni/La <sub>2</sub> O <sub>3</sub> metal–support interactions. Catalysis Science and Technology, 2016, 6, 3449-3456.	2.1	24
123	Organometal halide perovskite solar cells: degradation and stability. Energy and Environmental Science, 2016, 9, 323-356.	15.6	1,457
124	An Efficiency Evaluation of the EU's Allocation of Carbon Emission Allowances. Energy Sources, Part B: Economics, Planning and Policy, 2015, 10, 192-200.	1.8	50
125	Photoelectrochemical water splitting at low applied potential using a NiOOH coated codoped (Sn, Zr) α-Fe <sub>2</sub> O <sub>3</sub> photoanode. Journal of Materials Chemistry A, 2015, 3, 5949-5961.	5.2	211
126	Improved Raman and photoluminescence sensitivity achieved using bifunctional Ag@SiO <sub>2</sub> nanocubes. Physical Chemistry Chemical Physics, 2015, 17, 21226-21235.	1.3	30

#	Article	IF	CITATIONS
127	Efficient photoelectrochemical water splitting using three dimensional urchin-like hematite nanostructure modified with reduced graphene oxide. Journal of Power Sources, 2015, 287, 119-128.	4.0	94
128	Heterostructured Cu <sub>2</sub> O/CuO decorated with nickel as a highly efficient photocathode for photoelectrochemical water reduction. Journal of Materials Chemistry A, 2015, 3, 12482-12499.	5.2	257
129	Operando X-ray diffraction and X-ray absorption studies of the structural transformation upon cycling excess Li layered oxide Li[Li <sub>1/18</sub> Co <sub>1/6</sub> Ni <sub>1/3</sub> Mn <sub>4/9</sub> ]O <sub>2</sub> in Li ion batteries. lournal of Materials Chemistry A. 2015. 3. 8613-8626.	5.2	14
130	Facile one-pot controlled synthesis of Sn and C codoped single crystal TiO2 nanowire arrays for highly efficient photoelectrochemical water splitting. Applied Catalysis B: Environmental, 2015, 163, 478-486.	10.8	55
131	Trimetallic (Aurod-Pdshell-Ptcluster) Catalyst Used as Amperometric Hydrogen Peroxide Sensor. Biosensors, 2014, 4, 461-471.	2.3	1
132	Raman Scattering Surface Signal Enhancement: Induced by Au@SiO2 core-shell nanoclusters and nanorods IEEE Nanotechnology Magazine, 2014, 8, 29-36.	0.9	0
133	Water-based chemical synthesis of low cost CIGS thin films. Materials Research Innovations, 2014, 18, 430-435.	1.0	0
134	Hierarchical Copperâ€Decorated Nickel Nanocatalysts Supported on La <sub>2</sub> O <sub>3</sub> for Lowâ€Temperature Steam Reforming of Ethanol. ChemSusChem, 2014, 7, 570-576.	3.6	18
135	Bimetallic catalyst of PtIr nanoparticles with high electrocatalytic ability for hydrogen peroxide oxidation. Sensors and Actuators B: Chemical, 2014, 190, 55-60.	4.0	34
136	Synthesis of Ti0.7Mo0.3O2 supported-Pt nanodendrites and their catalytic activity and stability for oxygen reduction reaction. Applied Catalysis B: Environmental, 2014, 154-155, 183-189.	10.8	33
137	The development of highly crystalline single-phase Bi20TiO32 nanoparticles for light driven oxygen evolution. Applied Catalysis B: Environmental, 2014, 150-151, 363-369.	10.8	17
138	Functional palladium tetrapod core of heterogeneous palladium–platinum nanodendrites for enhanced oxygen reduction reaction. Journal of Power Sources, 2014, 251, 393-401.	4.0	9
139	Direct <i>In situ</i> Observation of Li <sub>2</sub> O Evolution on Li-Rich High-Capacity Cathode Material, Li[Ni <sub><i>x</i>/i&gt;/sub&gt;Li<sub>(1–2<i>x</i>)/3</sub>Mn<sub>(2–<i>x</i>)/3</sub>]O<sub>2</sub> (0</sub>	≥ <sup>6</sup> ⊺j ET	Qq <sup>39</sup> 3 0.784
140	Self-focusing Au@SiO <sub>2</sub> nanorods with rhodamine 6G as highly sensitive SERS substrate for carcinoembryonic antigen detection. Journal of Materials Chemistry B, 2014, 2, 629-636.	2.9	66
141	Composition-controlled optical properties of colloidal CdSe quantum dots. Applied Surface Science, 2014, 322, 177-184.	3.1	16
142	Novel Ag/Au/Pt trimetallic nanocages used with surface-enhanced Raman scattering for trace fluorescent dye detection. Journal of Materials Chemistry B, 2014, 2, 5550-5557.	2.9	43
143	The synergetic effect of graphene on Cu <sub>2</sub> O nanowire arrays as a highly efficient hydrogen evolution photocathode in water splitting. Journal of Materials Chemistry A, 2014, 2, 18383-18397.	5.2	259
144	Amorphous precursor compounds for CuInSe2 particles prepared by a microwave-enhanced aqueous synthesis and its electrophoretic deposition. CrystEngComm, 2014, 16, 3121-3127.	1.3	5

#	Article	IF	CITATIONS
145	Oxygen Vacancy Engineering of Cerium Oxides for Carbon Dioxide Capture and Reduction. ChemSusChem, 2013, 6, 1326-1329.	3.6	49
146	Pd/NiO core/shell nanoparticles on La0.02Na0.98TaO3 catalyst for hydrogen evolution from water and aqueous methanol solution. International Journal of Hydrogen Energy, 2013, 38, 13529-13540.	3.8	38
147	Dendritic platinum-decorated gold nanoparticles for non-enzymatic glucose biosensing. Journal of Materials Chemistry B, 2013, 1, 5925.	2.9	24
148	Comprehensive study of an air bleeding technique on the performance of a proton-exchange membrane fuel cell subjected to CO poisoning. Journal of Power Sources, 2013, 242, 264-272.	4.0	37
149	Au@SiO <sub>2</sub> core/shell nanoparticle assemblage used for highly sensitive SERSâ€based determination of glucose and uric acid. Journal of Raman Spectroscopy, 2013, 44, 1671-1677.	1.2	50
150	Highly efficient synthesis of reduced graphene oxide–Nafion nanocomposites with strong coupling for enhanced proton and electron conduction. RSC Advances, 2013, 3, 23212.	1.7	43
151	Preparation of highly dispersed catalytic Cu from rod-like CuO–CeO2 mixed metal oxides: suitable for applications in high performance methanol steam reforming. Catalysis Science and Technology, 2012, 2, 807.	2.1	27
152	Ultrathin TiO2-coated MWCNTs with excellent conductivity and SMSI nature as Pt catalyst support for oxygen reduction reaction in PEMFCs. Journal of Materials Chemistry, 2012, 22, 20977.	6.7	114
153	Soft X-ray Absorption Spectroscopic and Raman Studies on Li <sub>1.2</sub> Ni <sub>0.2</sub> Mn <sub>0.6</sub> O <sub>2</sub> for Lithium-Ion Batteries. Journal of Physical Chemistry C, 2012, 116, 25242-25247.	1.5	87
154	An Electrochemical Approach for Estimation of Intrinsic Active Area and Activation of Pt/C Nanoâ€catalysts. Journal of the Chinese Chemical Society, 2012, 59, 1303-1312.	0.8	3
155	Advanced nanoelectrocatalyst for methanol oxidation and oxygen reduction reaction, fabricated as one-dimensional pt nanowires on nanostructured robust Ti0.7Ru0.3O2 support. Nano Energy, 2012, 1, 687-695.	8.2	40
156	Enhanced hydrogen generation by cocatalytic Ni and NiO nanoparticles loaded on graphene oxide sheets. Journal of Materials Chemistry, 2012, 22, 13849.	6.7	127
157	Photocatalytic hydrogen production on nickel-loaded LaxNa1â^'xTaO3 prepared by hydrogen peroxide-water based process. Green Chemistry, 2011, 13, 1745.	4.6	75
158	Robust non-carbon Ti0.7Ru0.3O2 support with co-catalytic functionality for Pt: enhances catalytic activity and durability for fuel cells. Energy and Environmental Science, 2011, 4, 4194.	15.6	99
159	Investigation of Formation Mechanism of Pt(111) Nanoparticle Layers Grown on Ru(0001) Core. Langmuir, 2011, 27, 1131-1135.	1.6	7
160	Nanostructured Ti <sub>0.7</sub> Mo <sub>0.3</sub> O <sub>2</sub> Support Enhances Electron Transfer to Pt: High-Performance Catalyst for Oxygen Reduction Reaction. Journal of the American Chemical Society, 2011, 133, 11716-11724.	6.6	371
161	Characterization of K4Nb6O17synthesized by a sol–gel method for H2evolution. Journal of the Chinese Institute of Engineers, Transactions of the Chinese Institute of Engineers,Series A/Chung-kuo Kung Ch'eng Hsuch K'an, 2011, 34, 3-9.	0.6	4
162	Controlled Synthesis of CdSe Quantum Dots by a Microwaveâ€Enhanced Process: A Green Approach for Mass Production. Chemistry - A European Journal, 2011, 17, 5737-5744.	1.7	44

#	Article	IF	CITATIONS
163	Preparation of nano-sized Cu from a rod-like CuFe2O4: Suitable for high performance catalytic applications. Applied Catalysis B: Environmental, 2011, 106, 650-656.	10.8	53
164	Green fabrication of La-doped NaTaO3 via H2O2 assisted sol–gel route for photocatalytic hydrogen production. Applied Catalysis B: Environmental, 2011, 102, 343-351.	10.8	66
165	Chemical Dealloying Mechanism of Bimetallic Pt–Co Nanoparticles and Enhancement of Catalytic Activity toward Oxygen Reduction. Chemistry - A European Journal, 2010, 16, 4602-4611.	1.7	96
166	Structural and Electronic Effects of Carbonâ€Supported Pt <sub><i>x</i></sub> Pd <sub>1â^'<i>x</i></sub> Nanoparticles on the Electrocatalytic Activity of the Oxygenâ€Reduction Reaction and on Methanol Tolerance. Chemistry - A European Journal, 2010, 16, 11064-11071.	1.7	37
167	Effect of the Compact TiO <sub>2</sub> Layer on Charge Transfer between N3 Dyes and TiO <sub>2</sub> Investigated by Raman Spectroscopy. Journal of Physical Chemistry C, 2010, 114, 3185-3189.	1.5	39
168	Rapid Microwave-Enhanced Solvothermal Process for Synthesis of CuInSe <sub>2</sub> Particles and Its Morphologic Manipulation. Chemistry of Materials, 2010, 22, 4185-4190.	3.2	64
169	A novel architecture of poly(tetrafluoroethylene)-framed TiO2 electrodes for dye-sensitized solar cells. Electrochemistry Communications, 2009, 11, 1647-1649.	2.3	4